ISSN 0965-5441, Petroleum Chemistry, 2021, Vol. 61, No. 4, pp. 516–526. © The Author(s), 2021. This article is an open access publication.
Russian Text © The Author(s), 2021, published in Neftekhimiya, 2021, Vol. 61, No. 3, pp. 418–429.

Combined Synthesis and Hydroprocessing of Hydrocarbons over $Co/SiO_2 + ZSM\text{-}5 + Al_2O_3$ Catalysts Promoted by Nickel

R. E. Yakovenko[a],*, I. N. Zubkov[a], V. G. Bakun[a], and A. P. Savost'yanov[a]

[a] *Platov South Russian State Polytechnic University, Novocherkassk, Rostov oblast, 346428 Russia*
**e-mail: jakovenko39@gmail.com*

Received May 12, 2020; revised February 1, 2021; accepted March 18, 2021

Abstract—The study investigates the effects of nickel introduction methods on the properties of a hybrid cobalt catalyst in a combination of Fischer–Tropsch synthesis and the hydroprocessing of the synthesized products. At 240°C, 2 MPa, and syngas WHSV 1000 h^{-1}, the catalytic performances were compared, the products were analyzed for the hydrocarbon and fractional compositions, and the characteristics of the synthesized fuels were determined. Among the catalysts differing in nickel introduction method, the sample with a nickel-containing zeolite component prepared by ion exchange was found to have the highest hydrogenation activity, while the sample with a metal component generated by joint cobalt/nickel introduction [Co/SiO_2 + Ni(i)/HZSM-5 + Al_2O_3] exhibited the highest isomerization activity.

Keywords: Fischer–Tropsch synthesis, hydroprocessing, hybrid cobalt catalyst, nickel, product composition, promotion, fuel properties

DOI: 10.1134/S096554412105008X

Of late, it has become increasingly relevant to search for alternative methods for producing engine fuels from non-petroleum raw materials. One such method is the GTL (gas-to-liquid) technology, which involves processing natural gas or associated petroleum gas into synthetic liquid fuels (SLF) [1, 2]. The key GTL process step, namely the Fischer–Tropsch (FT) synthesis, is a complex catalytic process that produces a wide range of hydrocarbons (HCs) from a CO/H_2 mixture referred to as syngas. The HC range includes: C_1–C_4 (hydrocarbon gas), C_5–C_{10} (gasoline fuel), C_{11}–C_{18} (diesel fuel), C_{19}–C_{34} (paraffins or soft wax), and C_{35+} (ceresins or heavy wax). FT synthesis occurs in the presence of heterogeneous catalysts that contain group VIII metals (i.e., iron, cobalt, nickel, or ruthenium), and involves a complex combination of consecutive and parallel conversions [3].

In commercial practice, however, iron-based and cobalt-based catalysts have remained most in demand. Iron catalysts promote the formation of mostly alkenes (when under elevated pressure and temperature) or alcohols (at increased syngas hourly space velocity) [3, 4]. Chemicals synthesized over conventional cobalt FT catalysts, such as Co/SiO_2, Co/Al_2O_3, and Co/TiO_2, consist mostly of *n*-alkanes, the yield and composition of which are directly determined by process conditions [4, 5]. A high content of *n*-alkanes in the fuels (C_5–C_{18}) causes a low research octane number (RON 60) of the gasoline fuel and inadequate low-temperature properties of the diesel fuel (cloud point +5°C) which fail to meet the applicable regulations. To increase the proportion of branched alkanes in the synthesized fuels, natural gas liquids (NGLs) are hydroprocessed over zeolite catalysts in a hydrogen environment at 3–6 MPa [6].

Recent studies have focused on the development of bifunctional (hybrid) catalysts to produce high-performance fuels from CO and H_2 in one step [7–9]. These catalysts will combine the functions of HC synthesis (hydrogenating metals) and HC hydroprocessing (zeolites or zeolite-like structures that have a potential for oligomerization, hydrocracking, isomerization, aromatization, and hydrogenation of HCs under FT synthesis conditions [10, 11]). Researchers have faced a number of process challenges related to the creation and utilization of various forms of catalysts (composite or structured) [12]. These catalysts are classified according to the type of contact between FT synthesis sites and

acid active sites at the levels of reactor, of catalyst particle, and of active phase [12–17]. In terms of contact between active sites and of preparation methods, catalysts are grouped into supported [10, 18–25], encapsulated [10, 26, 27], and mixed catalysts. Catalysts of the last-mentioned type differ in the method for charging a pellet mixture [18, 19, 26, 28, 29] or comprise a pelletized mixture of components and binders [30, 31]. As noted in most studies, the production efficiency of fuel components correlates well with the proximity of FT synthesis sites to acid sites and can be adjusted by promotion.

Previously, we have developed a hybrid catalyst for one-step synthesis of fuel HCs from CO and H_2 [32, 33]. This catalyst represents a catalytic system prepared by mixing and subsequent powder molding of a cobalt-alumina-silica gel catalyst for FT synthesis [34], an HZSM-5 zeolite [35], and boehmite. Synthetic crude oil produced over this catalyst contains a large amount of alkenes (>40%), which have a negative impact on the performance of engine fuels. The content of unsaturated HCs can be reduced by introducing additional hydrogenating components, such as Pt, Pd, or Ni. Among these, nickel is the most attractive due to its availability and low cost. However, nickel exhibits intrinsic activity in FT synthesis, catalyzing mainly reactions that form light C_1–C_4 hydrocarbons. It has remained important to determine a proper method for introducing nickel into a hybrid catalyst to ensure that it selectively hydrogenates unsaturated HCs while being almost prevented from involvement in FT synthesis reactions.

Nickel is known to be unsuitable for the production of long-chain HCs in FT synthesis, and the nickel activity in the methanation reaction has been generally assumed to be mainly caused by the formation of metal carbonyls [36]. A review paper on the feasibility of nickel as an FT catalyst and promoter points out that the industrial operating conditions of most nickel catalysts are far from the optimal parameters of FT synthesis [37]. Nonetheless, new scientific avenues of inquiry and experimental abilities have increased the relevance of this research area [38, 39]. Advances have been made in finding novel methods for the preparation and activation of catalysts, in selecting operating conditions effective in the production of chemicals with the required hydrocarbon composition, and in developing novel catalysts including nickel-promoted ones. Researchers have considered bimetallic systems for selective production of mixed fuels with a minimized number of process steps [40, 41], as well as silica-gel-based cobalt-nickel systems, as promising components for bifunctional catalysts [42, 43]. Hybrid catalysts have also been considered, consisting, for example, of a cobalt-containing component and a Ni/ZSM-5 catalyst as a mixed layer or with layered catalyst charge [44].

This study investigates the effects of the method of nickel introduction into a Co/SiO_2 + ZSM-5 + Al_2O_3 hybrid catalyst on the activity and selectivity of this catalyst in the combined synthesis and hydroprocessing of HCs.

EXPERIMENTAL

Catalyst preparation. Hybrid catalysts were prepared by mixing powders (<100 μm) of a cobalt-containing component (35 wt %) and a ZSM-5 zeolite-containing component in the H-form (30 wt %) [35], as well as boehmite TH 80 (35 wt %) as a binder (the ZSM-5 manufactured by the Ishimbay Specialized Chemical Catalyst Plant, Republic of Bashkortostan, Russia; and the boehmite by Sasol). To plasticize the powder mixture, an aqueous-alcoholic solution of triethylene glycol with nitric acid was used. A nitric acid solution was prepared by introducing 1–2 mL of 65 wt % nitric acid into 90–100 mL of distilled water per 100 g of the powder mixture. Then triethylene glycol was added based on a nitric acid to triethylene glycol volumetric ratio of 1 : 3. Catalyst pellets were molded by extrusion, successively dried at room temperature for 24 h, at 80°C for 4 h, and at 100–150°C for 3 h, and calcined at 400°C for 4 h. The pellets were then ground to 1–2 mm particles. The catalysts prepared as described above had the following composition: 36.6 wt % cobalt/promoters, 36.6 wt % HZSM-5/nickel, and 26.8 wt % Al_2O_3.

The starting hybrid catalyst (Sample 1) consisted of Co/SiO_2 + HZSM-5 + Al_2O_3. Nickel was introduced into the promoted catalysts using three different methods: joint impregnation of silica gel with cobalt nitrate and nickel nitrate during the preparation of the cobalt-containing component (Sample 2: Co–Ni/SiO_2 + HZSM-5 + Al_2O_3); impregnation of HZSM-5 with a nickel nitrate solution (Sample 3: Co/SiO_2 + Ni/HZSM-5 + Al_2O_3); and ion exchange of the ZSM-5 ammonium form with a nickel nitrate solution [Sample 4: Co–Al_2O_3/SiO_2 + Ni(i)/HZSM-5 + Al_2O_3].

The cobalt-containing components included Co/SiO_2 (20.3–21.1 wt % Co with additional 1.0 wt % Al_2O_3) [34] developed for the synthesis of long-chain hydrocarbons,

Table 1. Physicochemical properties of the catalysts

Catalyst sample	Composition	Concentration, wt %		Particle size, nm		D^a, %
		Ni	Co	Co_3O_4	Co^0	
1	Co/SiO_2 + HZSM-5 + Al_2O_3	–	7.4	14.5	10.8	8.9
2	Co–Ni/SiO_2 + HZSM-5 + Al_2O_3	1.0	7.0	15.3	11.5	8.4
3	Co/SiO_2 + Ni/HZSM-5 + Al_2O_3	1.1	7.2	13.1	9.8	9.8
4	Co/SiO_2 + Ni(i)/HZSM-5 + Al_2O_3	0.3	7.1	14.0	10.4	9.2

[a] D is the dispersion of cobalt metal (Co^0).

and Co–Ni/SiO_2 (20.0 wt % Co and 1.0 wt % Ni). These were prepared by impregnation of *KSKG* grade silica gel (as per GOST 3956-76, manufactured by the Salavat Catalyst Plant, Republic of Bashkortostan, Russia) with a 55% cobalt nitrate solution. The former component was used to prepare Samples 1 and 2, and the latter for Samples 3 and 4 (Table 1). When aluminum or nickel was introduced along with cobalt, aluminum nitrate or nickel nitrate was respectively added to the cobalt nitrate impregnating solution, with the salt concentration determined on the basis of 1.0 wt % Al_2O_3 and Ni. The silica gel impregnation was carried out at 70–80°C for 0.5 h. Then the excess amount of the solution was removed, and wet catalyst pellets were heat-treated according to the following schedule: 80°C for 4 h, 100–150°C for 3 h, and 350°C for 4 h.

HZSM-5 was impregnated and heat-treated according to the procedure described above, using a 10% nickel nitrate solution. The zeolite's ammonium form was ion-exchanged with a 0.5 M nickel nitrate solution by the conventional procedure [45] at 60°C and under continuous stirring for 4 h. When the ion exchange was completed, the solution was filtered off, and the zeolite was washed with distilled water at 60°C. The wet HZSM-5 powder was heat-treated according to the following schedule: 80°C for 1 h, 150°C for 4 h, and 500°C for 4 h.

Examination of physicochemical and catalytic properties. The cobalt and nickel contents in the catalysts were determined by X-ray fluorescence (XRF) on an ARL QUANT'X spectrometer (Thermo Scientific, Switzerland) under the following conditions: air environment, Teflon support, effective irradiation area 48.99 mm^2.

The catalysts were analyzed by X-ray diffraction (XRD) on a Thermo Scientific ARL X'TRA powder diffractometer with monochromated CuK_α radiation using point-to-point scanning (step 0.01°, counting time 2 s) in the 2θ range of 5° to 80°. The qualitative phase composition was determined using the Crystallographica software and the PDF-2 database involved [46].

The X-ray patterns were processed using the FullProf software. The mean size of Co_3O_4 particles [$d(Co_3O_4)$, nm] for the characteristic line with 2θ = 36.8° was derived from the Scherrer equation [47]:

$$d(Co_3O_4) = \frac{K \cdot \lambda}{\beta \cdot \cos\theta},$$

where $d(Co_3O_4)$ is the mean particle size (nm); K is the dimensionless particle shape factor (K = 0.89); λ is the X-ray wavelength (nm); θ is the Bragg angle (rad); and β is the line broadening at half the maximum intensity (rad).

The size of cobalt particles was calculated by the formula [48]:

$$d(Co^0) = d(Co_3O_4) \cdot 0.75,$$

where $d(Co^0)$ is the size of cobalt particles (nm); and $d(Co_3O_4)$ is the size of cobalt oxide particles (nm).

The dispersion of the metal component (D, %) was determined by the formula [49]:

$$D = \frac{96}{d(Co^0)}.$$

Temperature-programmed reduction (TPR) of the catalysts was carried out using a Micromeritics ChemiSorb 2750 analyzer equipped with a thermal conductivity detector (TCD). A 0.1–0.15 g sample was placed into a quartz reactor installed in a heat-programmable oven. Prior to starting the TPR procedure, the catalyst sample was held under a He flow (20 mL/min) at 200°C for 1 h. Then it was cooled to room temperature, and a 10% H_2/90% N_2 mixture was introduced at 20 mL/min. The

examination was performed in the range of 20 to 800°C at a heating rate of 20°C/min.

The FT synthesis of HCs was carried out in a flow-through reactor with a stationary catalyst bed (10 cm^3) diluted with 30 cm^3 of quartz crumb at 2.0 MPa. Before starting the catalytic test, the samples were reduced under a hydrogen flow at 400°C and a gas hourly space velocity (WHSV) of 3000 h^{-1} for 1 h. Then the catalysts were activated by syngas (H_2/CO = 2) at 2.0 MPa and WHSV 1000 h^{-1} by stepwise temperature elevation (2.5°C/h) from 180 to 240°C. The balance tests were run at a constant temperature of 240°C (with a temperature gradient across the catalyst bed up to 3°C), 2.0 MPa, and WHSV 1000 h^{-1} for 70–90 h of continuous operation. The reproducibility of the experimental data was ensured by the metrological control of the process parameters that were implemented during the test, and by the duration of the examination. The material balance calculation error was within a margin of 3%.

The composition of gaseous synthetic products was analyzed by gas adsorption chromatography on a Crystal 5000 chromatograph (Chromatec, Russia) equipped with a thermal conductivity detector and two columns. One column, Haysep R (helium carrier gas, flow rate 15 mL/min), was used to analyze C_1–C_5 hydrocarbons and CO_2; the other column, NaX molecular sieves (argon carrier gas, flow rate 15 mL/min), was intended to analyze CO, H_2, and N_2. The heating was programmed at a rate of 8°C/min.

The C_{5+} HC composition was identified by capillary gas-liquid chromatography-mass spectrometry using an Agilent-US GC 7890 gas chromatograph equipped with an Agilent 5975C quadrupolar mass-selective detector (electron impact ionization mode, 70 eV) and an HP-5-MS capillary column (30 m × 0.25 mm × 0.25 μm, helium carrier gas). The gasoline, diesel, and paraffin products were analyzed by varying the column operating modes, the evaporator and thermostat temperatures, the gas pressure, the gas WHSV, and the programmed heating conditions.

The condensed synthetic chemicals were distilled at atmospheric pressure into a low-boiling distillate (180°C, LB), a high-boiling distillate (180–330°C, HB), and a bottom residue (>330°C). The filterability limit temperature of the diesel fuel was measured on a PTF-LAB-12 automatic instrument as per GOST 22254-92.

The cetane index was calculated according to ISO 4264:2018, "Petroleum Products: Calculation of Cetane Index of Middle-Distillate Fuels by the Four Variable Equation."

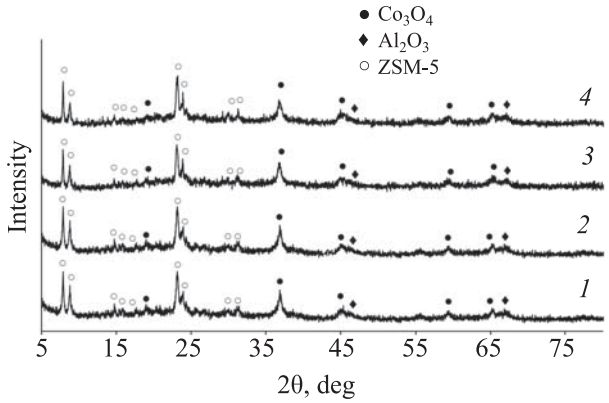

Fig. 1. X-ray patterns of catalysts: (*1*) Co/SiO_2 + HZSM-5 + Al_2O_3; (*2*) Co–Ni/SiO_2 + HZSM-5 + Al_2O_3; (*3*) Co/SiO_2 + Ni/HZSM-5 + Al_2O_3; (*4*) Co/SiO_2 + Ni(i)/HZSM-5 + Al_2O_3.

RESULTS AND DISCUSSION

Catalyst properties. Table 1 presents the compositions and physicochemical properties of the hybrid catalysts under study. The cobalt content in the samples ranges between 7.1 and 7.4 wt %.

The XRD examination of the catalysts in the oxide form demonstrated similar XRD patterns for all the samples (Fig. 1). The oxide precursor of the active component contains Co_3O_4 with a cubic spinel structure (*Fd*3*m*), which was detected as a number of crystalline phase reflections in the 2θ range of 18°–68°. Although, given the small amount of nickel, no Al_2O_3 or NiO phases crystallizing as a cubic spinel [46] were detected, these could potentially be present in the catalysts. Moreover, the formation of mixed oxide phases is typical for these metals. In view of the similarity of the crystalline structures of Co_3O_4, Al_2O_3, and NiO and the mixed structures like $NiCo_2O_4$ [50], and knowing the proximity of the corresponding diffraction peaks, it is always difficult to identify them in the catalyst structure. As a consequence, the Co_3O_4 structure may be distorted, which increases the defectiveness of the catalyst structures and contributes to the emergence of new catalytic sites; SiO_2 is X-ray amorphous. Reflections of ZSM-5 were observed between 2° and 12°. An alumina phase resulting from the thermal decomposition of boehmite is represented by reflections at 20.3°, 29.5°, and 52.0°. The cobalt particle size in the starting catalyst derived from the Scherrer equation is 10.8 nm. The introduction of nickel along with cobalt into the metal component enlarges the cobalt

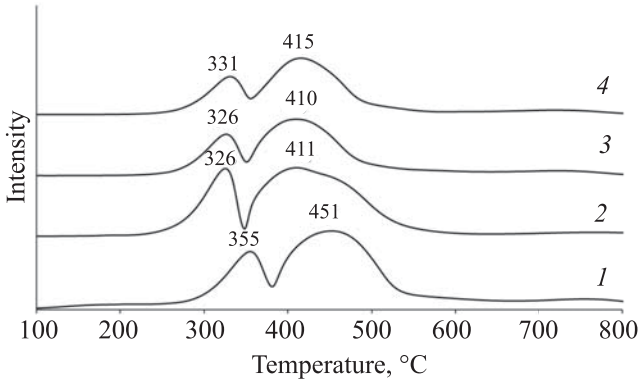

Fig. 2. TPR spectra of catalysts: (*1*) Co/SiO_2 + HZSM-5 + Al_2O_3; (*2*) Co–Ni/SiO_2 + HZSM-5 + Al_2O_3; (*3*) Co/SiO_2 + Ni/HZSM-5 + Al_2O_3; (*4*) Co/SiO_2 + Ni(i)/HZSM-5 + Al_2O_3.

particles up to 11.5 nm, while its introduction into the zeolite component reduces the cobalt particle size.

The surface phases formed during the catalyst reduction were identified by TPR (Fig. 2). The TPR spectra of all the catalysts display two major reduction peaks with maxima in the ranges of 321–355°C and 393–451°C. These peaks are attributed to the consecutive reduction of Co_3O_4 to cobalt metal (Co^0) [51] according to Eqs. (1) and (2), and are designated as peak 1 ($Co_3O_4 \rightarrow CoO$) and peak 2 ($CoO \rightarrow Co^0$), respectively:

$$Co_3O_4 + H_2 \rightarrow 3CoO + H_2O, \quad (1)$$

$$CoO + H_2 \rightarrow Co^0 + H_2O. \quad (2)$$

The introduction of nickel into the hybrid catalysts was found to intensify the process by lowering the catalyst reduction temperature (Table 2). The temperature maxima of peaks 1 and 2 in the TPR spectra of Samples 2–4 decline by 25–30°C and 35–40°C, respectively. The nickel introduction method does not have a significant effect, although peak 2 of Sample 4 is slightly shifted towards the high-temperature region. Similar regularities were also found in prior studies [52, 53].

The catalytic test of the FT catalyst samples was carried out at 240°C, 2 MPa, and WHSV 1000 h^{-1}. The test performance data are presented in Table 3.

All the catalysts are active in FT synthesis, with the CO conversion rate varying between 70.9% and 77.4%. The introduction of nickel into Sample 2 (along with cobalt) and into Sample 3 (prepared by zeolite impregnation) slightly decreases the C_{5+} selectivity and productivity of these catalysts, while it increases their selectivity for gaseous C_1–C_4 hydrocarbons. Obviously, in this case nickel exhibits intrinsic activity in FT synthesis, mostly catalyzing the formation of gaseous hydrocarbons. This activity is especially pronounced when nickel is introduced into the cobalt-containing component.

The highest C_{5+} productivity was reached by Sample 4, with nickel introduced into HZSM-5 by ion exchange. The productivity rise in the context of some decline in the selectivity for gaseous synthetic chemicals indicates the promoting effect of nickel in the catalytic system prepared in this manner, even at a considerably

Table 2. Temperature maxima in TPR spectra of catalyst samples

Catalyst sample	Peak 1		Peak 2		S_2/S_1
	temperature, °C	area S_1, %	temperature, °C	area S_2, %	
1. Co/SiO_2 + HZSM-5 + Al_2O_3	355	27.0	451	73.0	2.70
2. Co–Ni/SiO_2 + HZSM-5 + Al_2O	326	28.3	411	71.7	2.53
3. Co/SiO_2 + Ni/HZSM-5 + Al_2O_3	326	26.4	410	73.6	2.79
4. Co/SiO_2 + Ni(i)/HZSM-5 + Al_2O_3	331	28.1	415	71.9	2.56

Table 3. Test performance of FT catalysts

Catalyst sample	CO conversion rate, %	Selectivity, %				Productivity, kg/(m^3_{cat}·h)
		CH_4	C_2–C_4	C_{5+}	CO_2	
1. Co/SiO_2 + HZSM-5 + Al_2O_3	75.6	18.7	11.9	67.1	2.3	106.0
2. Co–Ni/SiO_2 + HZSM-5 + Al_2O	70.9	19.4	14.6	62.9	3.1	89.5
3. Co/SiO_2 + Ni/HZSM-5 + Al_2O_3	71.4	18.7	13.3	66.2	1.9	99.1
4. Co/SiO_2 + Ni(i)/HZSM-5 + Al_2O_3	77.4	18.5	10.7	68.2	2.6	111.0

Table 4. Group and fractional compositions of C_{5+} hydrocarbons

Catalyst sample	HC group	HC fractions, wt %			**Total**	*iso*/*n*[a]	O/P[b]
		C_5–C_{10}	C_{11}–C_{18}	C_{19+}			
1. $Co/SiO_2 + HZSM\text{-}5 + Al_2O_3$	*n*-Alkanes	12.5	18.4	5.2	36.1	0.76	0.72
	iso-Alkanes	9.5	10.8	1.7	22.0		
	Alkenes	18.3	2.3	–	20.6		
	Branched alkenes	14.0	7.3	–	21.3		
	Total	**54.3**	**38.8**	**6.9**	**100**		
2. $Co–Ni/SiO_2 + HZSM\text{-}5 + Al_2O_3$	*n*-Alkanes	15.7	14.2	7.3	37.2	1.18	0.51
	iso-Alkanes	14.5	13.0	1.6	29.1		
	Alkenes	7.8	0.9	–	8.7		
	Branched alkenes	19.7	5.3	–	25.0		
	Total	**57.7**	**33.4**	**8.9**	**100**		
3. $Co/SiO_2 + Ni/HZSM\text{-}5 + Al_2O_3$	*n*-Alkanes	13.5	25.5	8.1	47.1	0.73	0.50
	iso-Alkanes	6.4	10.9	2.1	19.4		
	Alkenes	8.1	2.6	–	10.7		
	Branched alkenes	13.5	9.3	–	22.8		
	Total	**41.5**	**48.3**	**10.2**	**100**		
4. $Co/SiO_2 + Ni(i)/HZSM\text{-}5 + Al_2O_3$	*n*-Alkanes	18.6	20.9	7.0	46.5	0.70	0.45
	iso-Alkanes	7.2	11.9	3.2	22.3		
	Alkenes	9.7	2.7	–	12.4		
	Branched alkenes	11.8	7.0	–	18.8		
	Total	**47.3**	**42.5**	**10.2**	**100**		

[a] Isomeric to normal HC ratio.
[b] Olefin to paraffin ratio.

lower metal concentration (by a factor of 3 to 4 compared to the other catalysts).

When using conventional catalysts with cobalt supported by an oxide (Al_2O_3, SiO_2, or TiO_2), the olefin content in the synthesized chemicals is known to usually not exceed 5–10% [5]. However, the introduction of ZSM-5 into a catalyst dramatically enhances the alkene yield in the C_{5+} chemicals at 230–250°C. Such regularities have been identified by various researchers, for example in a study on a ZSM-5-containing hybrid catalyst in the presence of which the synthetic chemicals had an alkene/*n*-alkane ratio of 0.9 [9].

In the C_5 synthetic chemicals produced in the presence of the starting hybrid catalyst (Sample 1) and of the catalyst containing nickel as a part of its metal component (Sample 2), the content of *n*-alkanes is about 37% (Table 4). The total contents of variously-structured alkanes and alkenes for all nickel-containing catalysts are 66–68 and 32–34%, respectively. At the same time, Sample 2 is distinguished by the highest isomerization activity, as indicated by 1.3-fold and 1.2-fold higher amounts of newly-formed *iso*-alkanes and branched alkenes, respectively, than for the starting catalyst. Hydrocarbons synthesized over Samples 3 and 4 (with nickel in the zeolite-containing component) contain about 47% *n*-alkanes and the smallest amount of alkenes, and exhibit the lowest and very similar isomeric to normal HC ratios and olefin to paraffin ratios.

At optimal fuel compositions, the best FT synthesis performance was achieved in the presence of the catalyst promoted by nickel using ion exchange at a metal content of at least 0.3 wt %. It is reasonable to assume that ion exchange results in the uniform distribution of a small amount of ca-ions throughout the mass of the fine-dispersed zeolite, and the catalyst reduction forces the metal to migrate from the bulk of the zeolite crystals to their external surface, thus forming a Me^0 phase vigorously involved in the variety of reactions on the surface of the hybrid catalyst [18].

Table 5. Gibbs free energy for hydrogenation of *n*-alkenes (**1**) and *iso*-alkenes (**3**) based on quantum-chemical calculations in gaseous phase at 250°C and 2 MPa

R	$\Delta G_{(\mathbf{1}+H_2)\rightarrow\mathbf{2}}$, kcal/mol	$\Delta G_{(\mathbf{3}+H_2)\rightarrow\mathbf{4}}$, kcal/mol	$\Delta\Delta G^a$, kcal/mol
$-CH_3$	+16.1	–15.4	0.7
$-C_3H_7$	–16.1	–15.4	0.7
$-C_{10}H_{21}$	–16.0	–15.5	0.5

[a] $\Delta\Delta G = \Delta G_{(\mathbf{3}+H_2)\rightarrow\mathbf{4}} - \Delta G_{(\mathbf{1}+H_2)\rightarrow\mathbf{2}}$.

The gasoline (C_5–C_{10}) and diesel (C_{11}–C_{18}) HCs account for 90–93% of the synthetic chemicals for all the catalysts (Table 4). The contents of unsaturated HCs in the gasoline and diesel fuels for Sample 1 are 59 and 25%, respectively. The introduction of nickel (Sample 2) decreases the amount of normal and branched alkenes in the gasoline and diesel fuels by 20 and 25%, respectively, and decreases the olefin to paraffin ratio by a factor of 1.4. A significant change in the fractional composition can be observed for Sample 3: a 1.3-fold decline in the gasoline content and a dramatic increase in the contents of the diesel fuel and long-chain HCs (a 1.5-fold growth in C_{19+}). The highest hydrogenation activity was exhibited by Sample 4. When compared to Sample 1, the total amount of unsaturated HCs in Sample 4 declined by a factor of 1.3, including drops in the contents of normal and branched alkenes in the gasoline fuel by factors of 1.9 and 1.2, respectively.

Thus, concerning gasoline fuel, regardless of the specific nickel introduction method, the hydrogenation rate of unsaturated HCs with the normal carbon skeleton structure is higher than that of branched alkenes. The hydrogenation of normal alkenes is probably more advantageous in terms of thermodynamics.

To compare the probability of the hydrogenation of normal and branched alkenes with different numbers of carbon atoms in the molecule under FT synthesis conditions, we carried out quantum-chemical calculations of Gibbs free energy (Fig. 3, Table 5). The calculations were performed using the Gaussian'09 software package [54] in the approximation of the density functional theory [DFT B3LYP/6-311++G(2d,2p)] [55]. The nature of the stationary point on the potential energy surface (the local minimum) was confirmed by calculating the Hessian matrix at the same level of theory in the harmonic approximation. All the initial (1, 3) and optimized (2, 4) structures had only real frequencies.

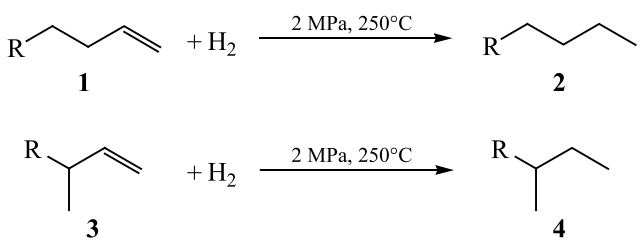

Fig. 3. Alkene hydrogenation under FT synthesis conditions.

The calculated Gibbs energies for the hydrogenation of normal and branched alkenes are similar (–16.1 and –15.4 kcal/mol). However, hydrogenation of normal alkenes is thermodynamically more advantageous. The Gibbs energies for the hydrogenation of alkenes with different carbon chain lengths are almost equal. Therefore, we can conclude that the composition of the synthesized chemicals is primarily determined by the catalyst selectivity.

The individual quality characteristics of the synthetic fuel hydrocarbons produced in the presence of Sample 4 were assessed for compliance with the Technical Regulation of the Customs Union (CU TR) no. 013/2011 [56]. The assessment data are presented in Tables 6 and 7.

In terms of the key environmental characteristics (contents of sulfur, benzene, and aromatic hydrocarbons), the synthesized gasoline fuel meets the CU TR specifications. However, because the olefin content significantly exceeds the applicable limit, this fuel needs to be additionally hydrogenated.

In terms of the characteristics relevant to the performance of internal combustion engines, including low-temperature properties, the synthesized diesel fuel meets the CU TR specifications. Moreover, this fuel is totally free of sulfur compounds and polycyclic aromatic hydrocarbons.

CONCLUSIONS

(1) It was found that the method for introducing nickel as a hydrogenating agent of the hybrid catalyst for combined FT synthesis and hydroprocessing of hydrocarbons has a decisive effect on the catalyst activity, as well as on the group composition and fractional composition of the synthetic chemicals. It was demonstrated that, to produce high-quality synthetic fuels, it is preferable to use a catalyst with nickel introduced into the zeolite-containing component by ion exchange (0.3 wt % nickel). At a CO conversion rate of 77.4%, the C_{5+} productivity of the catalyst (at 7.1 wt % cobalt)

Table 6. Quality characteristics of synthetic gasoline fuel (LB, –180°C)

Characteristics	CU TR specification (Class 5)	Actual
Sulfur (mg/kg), max	10	–
Benzene (vol %), max	1	–
HCs (vol %), max:		
aromatics	35	–
olefins	18	45

Table 7. Quality characteristics of synthetic diesel fuel (180–320°C)

Characteristics	CU TR specification (Class 5)	Actual
Sulfur (mg/kg), max	10	–
Closed-cup flash point (°C), min	30	57
Temperature of 95% of distilled volume (°C), max	360	315
Polycyclic aromatic HCs (wt %), max	8	–
Cetane number,[a] min	47	51
Cetane index	–	63
Filterability limit temperature (°C), max	–20	–21

[a] Qualitative estimate measured by SHATOX SX-300 Petroleum Quality Analyzer.

is 111.0 kg/(m^3_{cat} h). The introduction of nickel along with cobalt into the metal component decreases the C_{5+} productivity and selectivity of the catalyst as it promotes gas generation. This phenomenon appears to be caused by the intrinsic activity of nickel in FT synthesis.

(2) Regardless of the method employed, nickel introduction into the catalyst decreases the amount of unsaturated HCs in the synthetic chemicals (by a factor of 1.2–1.3 compared to the starting hybrid catalyst). In addition, its introduction into the cobalt-containing component also contributes to the catalyst's isomerization activity (as evidenced by the highest amounts of newly-formed *iso*-alkanes and branched alkenes). Hydrocarbons synthesized over catalysts with nickel in the zeolite-containing component are distinguished by the smallest alkene content and the lowest *iso/n* and olefin/paraffin ratios. The highest hydrogenation activity is achieved by the catalyst with nickel introduced by ion exchange (as evidenced by the 1.9- and 1.2-fold lower amounts of normal and branched alkenes, respectively). It is worth noting that the hydrogenation rate of normal unsaturated HCs in the gasoline fuel is higher than that of branched alkenes in the same.

(3) A series of quantum-chemical calculations were performed for the test conditions of the combined process under study. The calculations resulted in similar values of Gibbs free energy for the hydrogenation of normal and branched alkenes. However, hydrogenation of normal alkenes is thermodynamically more advantageous. The Gibbs energies for the hydrogenation of alkenes with different carbon chain lengths are almost equal. Thus, the composition of the synthetic chemicals is primarily determined by the catalyst selectivity.

(4) The synthetic fuel was assessed for compliance with the applicable Technical Regulation of the Customs Union (CU TR). The standardized characteristics of the diesel fuel were found to meet the CU TR specifications. Moreover, the diesel fuel is totally free of sulfur compounds and polycyclic aromatic HCs. The synthesized gasoline fuel meets the environmental specifications of the applicable CU TR, including the contents of sulfur, benzene, and aromatic HCs. However, this fuel requires minor hydrogenation to decrease the olefin content.

AUTHOR INFORMATION

R.E. Yakovenko, ORCID: http://orcid.org/0000-0001-9137-7265

I.N. Zubkov, ORCID: http://orcid.org/0000-0003-0828-3159

V.G. Bakun, ORCID: http://orcid.org/0000-0002-0971-8145

A.P. Savost'yanov, ORCID: http://orcid.org/0000-0002-5319-2443

FUNDING

The study described here was performed with financial support from the Russian Science Foundation (RSF grant no. 19-73-00089), using equipment of the Nanotechnology

Center for Collective Use, South Russian State Polytechnic University.

CONFLICT OF INTEREST

The authors declare no conflict of interest requiring disclosure in this article.

OPEN ACCESS

This article is licensed under a Creative Commons Attribution 4.0 International License, which permits use, sharing, adaptation, distribution and reproduction in any medium or format, as long as you give appropriate credit to the original author(s) and the source, provide a link to the Creative Commons licence, and indicate if changes were made. The images or other third party material in this article are included in the article's Creative Commons licence, unless indicated otherwise in a credit line to the material. If material is not included in the article's Creative Commons licence and your intended use is not permitted by statutory regulation or exceeds the permitted use, you will need to obtain permission directly from the copyright holder. To view a copy of this licence, visit http://creativecommons.org/licenses/by/4.0/.

REFERENCES

1. Arutyunov, V.S., Savchenko, V.I., Sedov, I.V., Nikitin, A.V., Troshin, K.Ya., Borisov, A.A., Fokin, I.G., Makaryan, I.A., and Strekova, L.N., *Eurasian Chem.-Technol. J*., 2017, vol. 19, pp. 265–271. https://doi.org/10.18321/ectj662
2. Tso, W.W., Niziolek, A.M., Onel, O., Demirhan, C.D., Floudas, C.A., and Pistikopoulos, E.N., *Comput. Chem. Eng*., 2018, vol. 113, pp. 222–239. https://doi.org/10.1016/j.compchemeng.2018.03.003
3. Khodakov, A.Y., Chu, W., and Fongarland, P., *Chem. Rev*., 2007, vol. 107, pp. 1692–1744. https://doi.org/10.1021/cr050972v
4. Krylova, A.Yu., *Khim. Tverd. Topliva*, 2014, no. 1, pp. 23–36.
5. Eliseev, O.L., Savost'yanov, A.P., Sulima, S.I., and Lapidus, A.L., *Mendeleev Commun*., 2018, vol. 28, no. 4, pp. 345–351. https://doi.org/10.1016/j.mencom.2018.07.001
6. Kikhtyanin, O.V. and Echevskii, G.V., *Katal. Prom–ti*, 2008, no. 3, pp. 47–53.
7. Sineva, I.V., Asalieva, E.Yu., and Mordkovich, V.Z., *Russ. Chem. Rev*., 2015, vol. 84, no. 11, pp. 1176–1189. https://doi.org/10.1070/RCR4464
8. Chunxiang, Z. and George, M.B., *Appl. Catal. B: Environmental*, 2018, vol. 235, pp. 92–102. https://doi.org/10.1016/j.apcatb.2018.04.063
9. Wang, Y., Zhao, W., Li, Z., Wang, H., Wu, J., Li, M., Hu, Z., Wang, Y., Huang, J., and Zhao, Y., *J. Porous Material*., 2015, vol. 22, pp. 339–345. https://doi.org/10.1007/s10934-014-9901-9
10. Sartipi, S., Parashar, K., Valero-Romero, M., Santos, V., Linden, B., Makkee, M., Kapteijn, F., and Gascon, J., *J. Catal*., 2013, vol. 305, pp. 179–190. https://doi.org/10.1016/j.jcat.2013.05.012
11. Sartipi, S., Makkee, M., Kapteijn, F., and Gascon, J., *Catal. Sci. Technol*., 2014, vol. 4, pp. 893–907. https://doi.org/10.1039/C3CY01021J
12. Martínez, A. and Prieto, G., *Topics in Catal*., 2009, vol. 52, pp. 75–90. https://doi.org/10.1007/s11244-008-9138-4
13. Zhang, Q., Cheng, K., Kang, J., Deng, W., and Wang, Y., *ChemSusChem*., 2014, vol. 7, pp. 1251–1264. https://doi.org/10.1002/cssc.201300797
14. Espinosa, G., Domingueza, J.M., Morales-Pachecob, P., Tobona, A., Aguilara, M., and Benitezam, J., *Catal. Today*, 2011, vol. 166, pp. 47–52. https://doi.org/10.1016/j.cattod.2011.01.025
15. Majewska, J. and Michalkiewicz, B., *Int. J. Hydrogen Energy*, 2016, vol. 41, no. 20, pp. 8668–8678. https://doi.org/10.1016/j.ijhydene.2016.01.097
16. Lee, D.-K., Kim, D.-S., Kim, T.-H., Lee, Y.-K., Jeong, S.-E., Le, N.T., Cho, M.-J., and Henam, S.D., *Catal. Today*, 2010, vol. 154, pp. 237–243. https://doi.org/10.1016/j.cattod.2010.03.053
17. Adeleke, A.A., Liu, X., Lu, X., Moyo, M., and Hildebrandtm, D., *Rev. Chem. Eng*., 2020, vol. 36, pp. 437–457. https://doi.org/10.1515/revce-2018-0012
18. Subramanian, V., Zholobenko, V., Cheng, K., Lancelot, C., Heyte, S., Thuriot, J., Paul, S., Ordomsky, V., and Khodakov, A., *ChemCatChem*., 2016, vol. 8, no. 2, pp. 380–389. https://doi.org/10.1002/cctc.201500777
19. Nakanishi, M., Uddin, Md.A., Kato, Y., Nishina, Y., and Hapipi, A.M., *Catal. Today*, 2017, vol. 291, pp. 124–132. https://doi.org/10.1016/j.cattod.2017.01.017
20. Velichkina, L.M., Vosmerikova, L.N., Korobitsyna, L.L., Kanashevich, D.A., Vosmerikov, A.V., and Abdiyusupov, G.G., *Nauch.-Tekhn. Dostizh. Pered. Opyt*, 2016, no. 1, pp. 13–19.
21. Sartipi, S., Parashar, K., Makkee, M., Gascon, J., and Kapteijn, F., *Catal. Sci. Technol*., 2013, vol. 3, pp. 572–575. https://doi.org/10.1039/C2CY20744C
22. Sartipi, S., Alberts, M., Meijerink, M.J., Keller, T.C., Prez-Ramrez, J., Gascon, J., and Kapteijn, F., *ChemSusChem*.,

2013, vol. 6, pp. 1646–1650.
https://doi.org/10.1002/cssc.201300339
23. Yao, M., Yao, N., Liu, B., Li, S., Xu, L., and Li, X., *Catal. Sci. Technol*., 2015, vol. 5, pp. 2821–2828.
https://doi.org/10.1039/C5CY00017C
24. Calleja, G., Lucas, A., and Grieken, R., *Fuel*, 1995, vol. 74, pp. 445–451.
https://doi.org/10.1016/0016-2361(95)93480-2
25. Dalil, M., Sohrabi, M., and Royaee, S.J., *J. Indust. Eng. Chem*., 2012, vol. 18, pp. 690–696.
https://doi.org/10.1016/j.jiec.2011.11.114
26. Lin, Q., Yang, G., Li, X., Yoneyama, Y., Wan, H., and Tsubaki, N., *ChemCatChem*., 2013, vol. 5, pp. 3101–3106.
https://doi.org/10.1002/cctc.201300336
27. Chunxiang, Z., George, M.B., *Appl. Catal. B: Environmental*., 2018, vol. 235, pp. 92–102.
https://doi.org/10.1016/j.apcatb.2018.04.063
28. Osa, A.R., Romero, A., Díez-Ramírez, J., Valverde, J.L., and Sánchez, P., *Topics in Catal*., 2017, vol. 60, pp. 1082–1093.
https://doi.org/10.1007/s11244-017-0792-2
29. Li, Z., Wu, L., Han, D., and Wu, J., *Fuel*, 2018, vol. 220, pp. 257–263.
https://doi.org/10.1016/j.fuel.2018.02.004
30. Kibby, C., Jothimurugesan, K., Das, T., Lacheen, H.S., Rea, T., and Saxton, R.J., *Catal. Today*, 2013, vol. 215, pp. 131–141.
https://doi.org/10.1016/j.cattod.2013.03.009
31. Cheng, S., Mazonde, B., Zhang, G., Javed, M., Dai, P., Cao, Y., Tu, S., Wu, J., Lu, C., Xing, C., and Shan, S., *Fuel*, 2018, vol. 223, pp. 354–359.
https://doi.org/10.1016/j.fuel.2018.03.042
32. Yakovenko, R.E., Zubkov, I.N., Narochnyi, G.B., Nekroenko, S.V., and Savost'yanov, A.P., *Katal. Prom–ti*, 2019, vol. 19, no. 3, pp. 178–186.
https://doi.org/10.18412/1816-0387-2019-3-178-186
33. Yakovenko, R.E., Narochnyi, G.B., Zubkov, I.N., Nepomnyashchikh, E.V., and Savost'yanov, A.P., *Kinet. Catal*., 2019, vol. 60, no. 2, pp. 212–220.
https://doi.org/10.1134/S0023158419020137
34. Savost'yanov, A.P., Yakovenko, R.E., Sulima, S.I., Bakun, V.G., Narochnyi, G.B., Chernyshev, V.M., and Mitchenko, S.A., *Catal. Today*, 2017, vol. 279, pp. 107–114.
https://doi.org/10.1016/j.cattod.2016.02.037
35. Shavaleev, D.A., Travkina, O.S., Alekhina, I.E., Ershtein, A.S., Basimova, R.A., and Pavlov, M.L., *Vest. Bashkir. Univ*., 2015, vol. 20, no. 1, pp. 58–65.
36. Dry, M.E., *Catal. Today*, 2002, vol. 71, nos. 3–4, pp. 227–241.
https://doi.org/10.1016/S0920-5861(01)00453-9
37. Enger, B.C. and Holmen, A., *Catal. Rev.: Sci. Eng*., 2012, vol. 54, no. 4, pp. 437–488.
https://doi.org/10.1080/01614940.2012.670088
38. Rytter, E., Skagseth, T.H, Eri, S., and Sjestad, A.O., *Ind. Eng. Chem. Res*., 2010, vol. 49, pp. 4140–4148.
https://doi.org/10.1021/ie100308f
39. Enger, B.C., Fossan, Å.-L., Borg, Ø., Rytter, E., and Holmen, A.P., *J. Catal*., 2011, vol. 284, no. 1, pp. 9–22.
https://doi.org/10.1016/j.jcat.2011.08.008
40. Feyz, M., Babakhanian, A., and Gholivand, M.B., *Korean J. Chem. Eng*., 2013, vol. 31, pp. 37–44.
https://doi.org/10.1007/s11814-013-0186-5
41. Calderone, V.R., Shiju, N.R., and Ferré, D.C., *GreenChem*., 2011, vol. 13, pp. 1950–1959.
https://doi.org/10.1039/C0GC00919A
42. Ramasamy, K.K., Gray, M., Job, H., and Wang, Y., *Chem. Eng. Sci*., 2015, vol. 135, pp. 266–273.
https://doi.org/10.1016/j.ces.2015.03.064
43. Sun, Y., Wei, J., Zhang, J.P., and Yang, G., *J. Natural Gas Sci. Eng*., 2016, vol. 28, pp. 173–183.
https://doi.org/10.1016/j.jngse.2015.11.008
44. Freitez, A., Pabst, K., Kraushaar-Czarnetzki, B., and Schaub, G., *Indust. Eng. Chem. Res*., 2011, vol. 50, pp. 13732–13741.
https://doi.org/10.1021/ie201913s
45. Alkhimov, S.A., Grigor'ev, D.A., and Mikhailov, M.N., *Katal. Prom–ti*, 2013, no. 4, pp. 16–20.
46. PDF-2. The powder diffraction file TM. International Center for Diffraction Data (ICDD). PDF-2 Release 2012.
https://www.icdd.com/pdf-2/.
47. Young, R.A., *The Rietveld Method*, Oxford: Oxford University Press, 1995.
48. Schanke, D., Vada, S., Blekkan, E.A., Hilmen, A.M., Hoff, A., and Holmen, A., *J. Catal*., 1995, vol. 156, pp. 85–95.
https://doi.org/10.1006/jcat.1995.1234
49. Xu, D., Li, W., Duan, H., Ge, Q., and Xu, H., *Catal. Lett*., 2005, vol. 102, pp. 229–235.
https://doi.org/10.1007/s10562-005-5861-7
50. Chang, J., Sun, J., Xu, C.H., Xu, H., and Gao, L., *Nanoscale*, 2012, vol. 4, pp. 6786–6791.
https://doi.org/10.1039/C2NR31725G
51. Pardo-Tarifa, F., Cabrera, S., Sanchez-Dominguez, M., and Boutonnet, M., *Int. J. Hydrogen Energy*, 2017, vol. 42,

no. 15, pp. 975–9765.
https://doi.org/10.1016/j.ijhydene.2017.01.056

52. Alkhimov, S.A., Grigor'ev, D.A., Mikhailov, M.N., *Katal. Prom–ti*, 2013, no. 4, pp. 31–41.
53. Martinelli, M., Karuturi, S.C., Garcia, R., Watson, C.D., Shafer, W.D., Cronauer, D.C., Kropf, A.J., Marshall, C.L., and Jacobs, G., *Catalysts*, 2020, vol. 10, pp. 334–338.
https://doi.org/10.3390/catal10030334
54. Frisch, M.J., Trucks, G.W., Schlegel, H.B., Scuseria, G.E., Robb, M.A., Cheeseman, J.R., Scalmani, G., Barone, V., Mennucci, B., Petersson, G.A., Nakatsuji, H., Caricato, M., Li, X., Hratchian, H.P., Izmaylov, A.F., Bloino, J., Zheng, G., Sonnenberg, J.L., Hada, M., Ehara, M., Toyota, K., Fukuda, R., Hasegawa, J., Ishida, M., Nakajima, T., Honda, Y., Kitao, O., Nakai, H., Vreven, T., Montgomery, J.A., Peral-ta, J.E., Ogliaro, F., Bearpark, M.J., Heyd, J., Brothers, E.N., Kudin, K.N., Staroverov, V.N., Kobayashi, R., Normand, J., Raghavachari, K., Rendell, A.P., Burant, J.C., Iyengar, S.S., Tomasi, J., Cossi, M., Rega, N., Millam, N.J., Klene, M., Knox, J.E., Cross, J.B., Bakken, V., Adamo, C., Jaramillo, J., Gomperts, R., Stratmann, R.E., Yazyev, O., Austin, A.J., Cammi, R., Pomelli, C., Ochterski, J.W., Martin, R.L., Morokuma, K., Zakrzewski, V.G., Voth, G.A., Salvador, P., Dannenberg, J.J., Dapprich, S., Daniels, A.D., Farkas, Ö., Foresman, J.B., Ortiz, J.V., Cioslowski, J., and Fox, D.J., *Gaussian 09*, Revision D.01 Gaussian, Inc., Wallingford, CT: USA, 2009.
55. Becke, A.D., *J. Chem. Phys*., 1993, vol. 98, pp. 5648–5652.
https://doi.org/10.1063/1.464913
56. *Tekhnicheskii reglament tamozhennogo soyuza (TR TS 013/2011) "O trebovaniyakh k avtomobil'nomu i aviatsionnomu benzinu, dizel'nomu i sudovomu toplivu, toplivu dlya reaktivnykh dvigatelei i mazutu" ot 18 oktyabrya 2011 g*. [Technical Regulations of the Customs Union (TR TS 013/2011) "On Requirements For Motor And Aviation Gasoline, Diesel And Marine Fuel, Jet Fuel And Fuel Oil" dated October 18, 2011].